JACS
JOURNAL OF THE AMERICAN CHEMICAL SOCIETY
Article
pubs.acs.org/JACS

Catalytic Reduction of N_2 to NH_3 by an Fe–N_2 Complex Featuring a C-Atom Anchor

Sidney E. Creutz and Jonas C. Peters*

Division of Chemistry and Chemical Engineering, California Institute of Technology, Pasadena, California 91125, United States

Supporting Information

ABSTRACT: While recent spectroscopic studies have established the presence of an interstitial carbon atom at the center of the iron–molybdenum cofactor (FeMoco) of MoFe-nitrogenase, its role is unknown. We have pursued Fe–N_2 model chemistry to explore a hypothesis whereby this C-atom (previously denoted as a light X-atom) may provide a flexible trans interaction with an Fe center to expose an Fe–N_2 binding site. In this context, we now report on Fe complexes of a new tris(phosphino)alkyl (CP^{iPr}_3) ligand featuring an axial carbon donor. It is established that the iron center in this scaffold binds dinitrogen trans to the C_{alkyl}-atom anchor in three distinct and structurally characterized oxidation states. Fe–C_{alkyl} lengthening is observed upon reduction, reflective of significant ionic character in the Fe–C_{alkyl} interaction. The anionic $(CP^{iPr}_3)FeN_2^-$ species can be functionalized by a silyl electrophile to generate $(CP^{iPr}_3)Fe–N_2SiR_3$. $(CP^{iPr}_3)FeN_2^-$ also functions as a modest *catalyst* for the reduction of N_2 to NH_3 when supplied with electrons and protons at −78 °C under 1 atm N_2 (4.6 equiv NH_3/Fe).

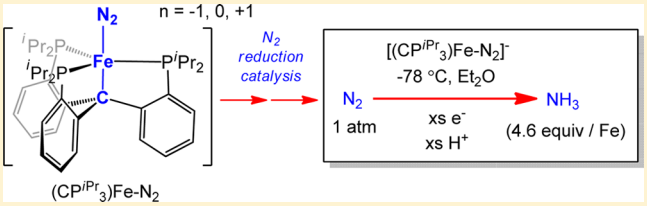

INTRODUCTION

The biological reduction of atmospheric N_2 to NH_3 is a fascinating yet poorly understood transformation that is essential to life.[1] The iron–molybdenum cofactor (FeMoco) of MoFe nitrogenase catalyzes N_2 reduction and has been extensively studied.[2] This cofactor has attracted the attention of inorganic and organometallic chemists for decades who have sought inspiration to explore the ability of synthetic iron and molybdenum complexes to bind and reduce dinitrogen.[3−6] Advances in the past decade have included two molybdenum systems that facilitate catalytic turnover of N_2 to NH_3 in the presence of inorganic acid and reductant sources,[7−9] and iron complexes that support a range of N_xH_y ligands relevant to nitrogen fixation,[10−13] effect reductive N_2 cleavage,[14,15] and facilitate N_2 functionalization.[16−18]

The presence of an interstitial light atom in the MoFe nitrogenase cofactor was established in 2002,[19] and structural, spectroscopic, and biochemical data have more recently established its identity as a C-atom.[20] The role of the C-atom is unknown. This state of affairs offers an opportunity for organometallic chemists to undertake model studies that can illuminate plausible roles for this interstitial C-atom, and hence critical aspects of the mechanism of N_2 reduction catalysis. In particular, Fe-alkyl complexes that are more ionic in nature than a prototypical transition metal–alkyl may be relevant to modeling the Fe–$C_{interstitial}$ interaction of the possible N_2 binding site in the cofactor (Figure 1).

We have suggested that a possible role played by the interstitial C-atom is to provide a flexible Fe–$C_{interstitial}$ interaction that exposes an Fe–N_2 binding site on a belt iron atom trans to the Fe–C linkage (Figure 1).[3,15,21−23]

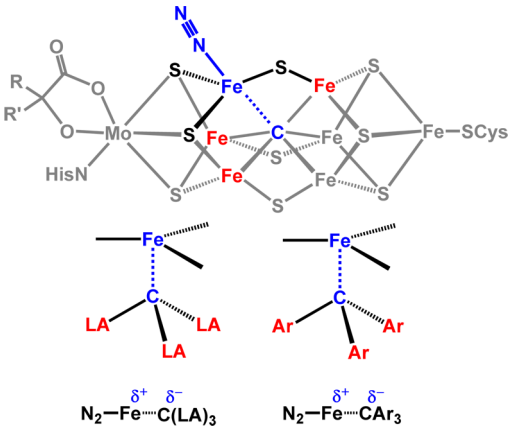

Figure 1. (Top) Structure of the FeMo cofactor of nitrogenase, showing a putative site for dinitrogen binding and highlighting the trigonal bipyramidal coordination environment at Fe. Possible sites of H-atoms on cofactor prior to N_2 binding not shown. (Bottom) Possible role of Lewis acidic (LA) or aryl substituents in stabilizing ionic character in the N_2–Fe–C_{alkyl} interaction.

Subsequent modulation of the Fe–C interaction and hence the local Fe geometry as a function of the N_2 reduction state might enable the Fe center to stabilize the various N_xH_y intermediates sampled along a pathway to NH_3.

To test the chemical feasibility of this hypothesis for Fe-mediated N_2 reduction, our group has previously employed phosphine-supported Fe complexes in approximately trigonal

Received: November 11, 2013

   dx.doi.org/10.1021/ja4114962 | J. Am. Chem. Soc. XXXX, XXX, XXX–XXX

geometries (pseudotetrahedral, trigonal pyramidal, or trigonal bipyramidal) to bind and functionalize dinitrogen. Tripodal trisphosphine ligands featuring an axial donor (X = N, Si, B) and aryl backbones have been used to canvass the ability of low-valent iron in such geometries to bind and activate dinitrogen (Figure 2).[23−25] The (TP^{iPr}B)Fe-system (TP^{R}B = tris(*o*-

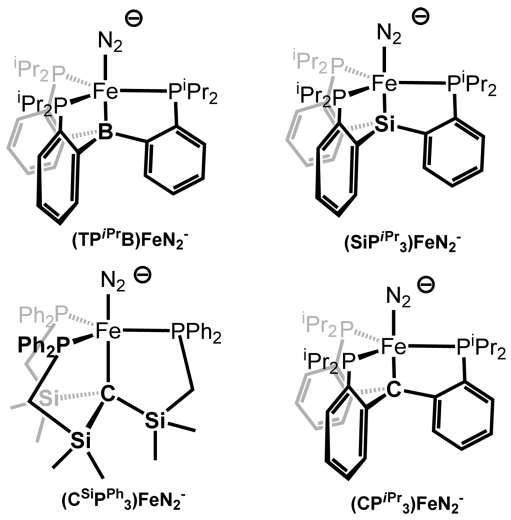

Figure 2. Select trigonal bipyramidal scaffolds previously studied by our lab, and the present (CP$^{iPr}_3$)FeN$_2^-$ system.

phosphinoaryl)borane) has proven rich in this context, and has most recently been shown to be a modestly effective catalyst for the reduction of N_2 to NH_3 in the presence of proton and electron sources at low temperature and 1 atm N_2.[21] An important feature of the (TP^{iPr}B)Fe-system is the presence of a flexible Fe−B interaction.[15,25] This flexibility may facilitate the formation of intermediates featuring Fe−N$_x$ π-bonding (e.g., Fe═NNH$_2$, Fe≡N, Fe═NH) during catalysis. Whether the aforementioned hypothesis concerning a hemilabile role for the interstitial C-atom of FeMoco is correct or not, these inorganic model studies lend credibility to the idea so far as the principles of coordination chemistry are concerned.

To extend our studies to systems that place a C-atom in a position trans to an Fe−N_2 binding site, we have sought related ligand scaffolds that feature a C-atom anchor. In designing these scaffolds, we have hypothesized that the proposed flexibility of the Fe−C linkage in the FeMo cofactor may be facilitated by the ability of the environment around the interstitial carbide—five additional electropositive Fe atoms—to stabilize developing negative charge on the carbon. With this in mind, we have previously reported iron complexes of a tris(phosphino)alkyl ligand whose axial carbon binding site is flanked by three electropositive silyl groups (Figure 2) which play a role in stabilizing the substantial ionic character of this Fe−C$_{alkyl}$ bond (Figure 1).[22]

Herein we report a new tris(phosphino)alkyl ligand, (CP$^{iPr}_3$), featuring aryl linkers bound to the axial carbon. We reasoned that possible delocalization of negative charge buildup into the aryl π-system would allow for increased flexibility in the Fe−C bond; this flexibility is expected to facilitate possible catalytic N_2 functionalization and reduction, as discussed above. Additionally, as this ligand is closely structurally related to the SiP$_3$, TPB, and NP$_3$ ligands whose iron coordination chemistry we have extensively explored, Fe complexes of CP$_3^{iPr}$ are of obvious comparative interest and would be particularly beneficial with regard to considering the role an Fe−C$_{interstitial}$ interaction might play in facilitating N_2 binding and reduction within the cofactor. To this end, we embarked on the synthesis of the new ligand (CP$^{iPr}_3$)H and the development of its Fe−N_2 chemistry.

RESULTS AND DISCUSSION

Ligand Synthesis. Whereas the ligands (SiP$^{iPr}_3$)H and TP^{iPr}B are straightforward to synthesize by the addition of lithiated *o*-phosphinophenyl precursors to $HSiCl_3$ and BCl_3,[24,26] the preparation of (CP$^{iPr}_3$)H via an analogous method by addition of phosphinoaryllithium moieties to a C_1 source (e.g., triple addition to dimethylcarbonate followed by deoxygenation of the resultant triarylmethanol product) has proven ineffective in our hands. However, an orthogonal synthetic approach based on elaboration of an initially formed triarylmethane scaffold afforded a viable approach to the preparation of (CP$^{iPr}_3$)H on a multigram scale and in reasonable yields. This synthesis of (CP$^{iPr}_3$)H follows an approach inspired by a previously reported synthesis of Ph$_2$P(*o*-C$_6$H$_4$CH$_2$C$_6$H$_4$-*o*)PPh$_2$,[27] and hinges on the sequential formation and cleavage of two diaryliodonium ions to give the tris(2-halophenyl)methane precursor (**5**) (Scheme 1).

Scheme 1. Synthesis of (CP$^{iPr}_3$)H (1)

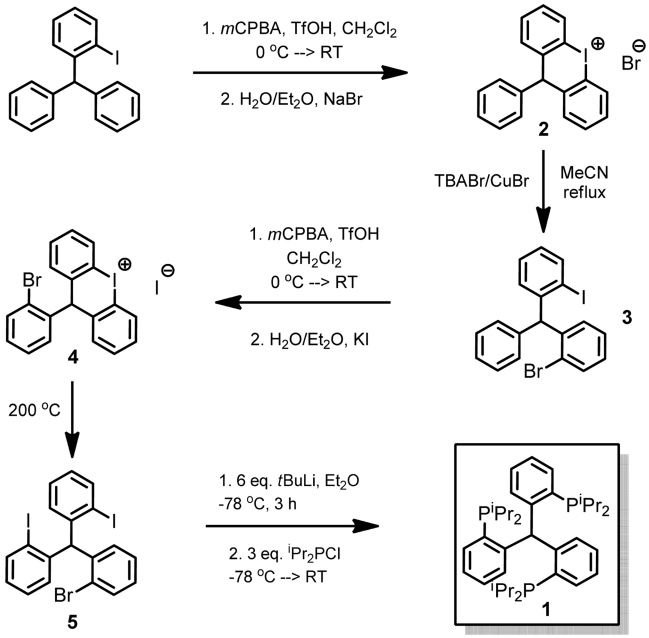

The synthesis of *o*-iodotriphenylmethane has been previously reported[28] and is readily effected in three steps from commercially available 2-nitrobenzaldehyde on a 20-g scale. Cyclization of this species to the diaryliodonium bromide salt (**2**) is accomplished by a previously reported technique.[29] Slow but clean ring-opening of **2** by CuBr and [TBA][Br] in acetonitrile gives 2-bromo-2′-iodotriphenylmethane (**3**). The 2-bromo-2′-iodotriphenylmethane species was targeted rather than 2,2′-diiodotriphenylmethane in order to mitigate the possibility of complications from excessive oxidation in the next step.

Formation of a second diaryliodonium cation as its iodide salt follows via an analogous procedure to regioselectively generate **4**, which can be straightforwardly decomposed to 2-bromo-2′,2″-diiodotriphenylmethane (**5**) by heating to 200 °C

dx.doi.org/10.1021/ja4114962 | J. Am. Chem. Soc. XXXX, XXX, XXX−XXX

for 15 min under an inert atmosphere. Each step in the synthesis of **5** from *o*-iodotriphenylmethane can be accomplished in 75% yield or more (overall yield: 38% over five steps).

Lithiation of **5** with 6 equiv of *tert*-butyllithium at −78 °C followed by treatment with 3 equiv of diisopropylphosphine chloride gives the desired tris(*o*-diisopropylphosphinophenyl)-methane, $(CP^{iPr}_3)H$ (**1**) in 67% yield (Scheme 1). The protonated form of the ligand, **1**, is characterized by a single peak in its phosphorus NMR spectrum at −9.1 ppm. The ^1H NMR spectrum, while indicative of 3-fold symmetry, also shows features suggestive of a rigid ligand scaffold where rotation about the phosphine-carbon bonds is hindered; in particular, four magnetically inequivalent sets of resonances are observed for the isopropyl methyl hydrogens. Additionally, the central C−H methine proton is shifted markedly downfield (8.15 ppm) and manifests as a quartet due to through-space coupling to the three phosphorus atoms. Similar NMR properties were observed for the central methine proton in a related trisphosphine ligand based on a tris(indolyl)methane scaffold.[30]

Metalation at Iron and Precursor Complexes. We initially hoped to effect metalation of **1** by first deprotonating it to give an alkali metal complex followed by transmetalation with an iron(II) halide or other transition metal precursor. To our frustration, **1** proved unexpectedly difficult to deprotonate even with very strong bases such as benzyl potassium and Schlosser's base,[31] perhaps due in part to the steric protection of the methine proton; additionally, the acidity of this proton is likely not as high as for bare triphenylmethane since the ligand bulk limits the extent to which the aryl rings can approach a coplanar configuration to afford resonance stabilization of a resulting carbanion.[32] Furthermore, the strategy used for metalation of the $(SiP^{iPr}_3)H$ ligand on iron—using methyl Grignard with $FeCl_2$ to generate a methyl iron complex which then eliminates methane with concomitant formation of the iron−silicon bond[24]—was not effective for $(CP^{iPr}_3)H$. It appeared to instead result in reduction of iron without the formation of the desired iron−carbon bond. Thus, it was necessary to develop a different protocol for the formation of a (CP^{iPr}_3)Fe-complex featuring an iron−carbon bond.

Combining **1** and iron(II) iodide in toluene cleanly affords the tetracoordinate, κ_2-bisphosphine diiodide high-spin iron(II) complex (**6**) as a yellow powder (Scheme 2). Its solid-state structure (Figure 3) shows a tetrahedral environment at the iron center and a bidentate binding mode for the ligand. One-

Scheme 2. Synthesis of Iron Complexes of $(CP^{iPr}_3)H$

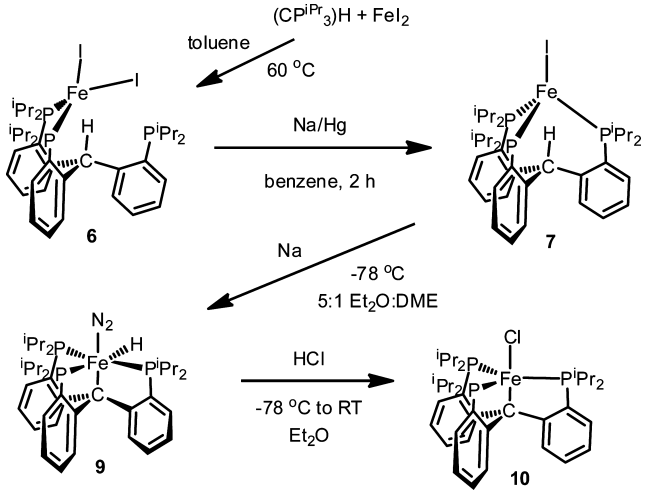

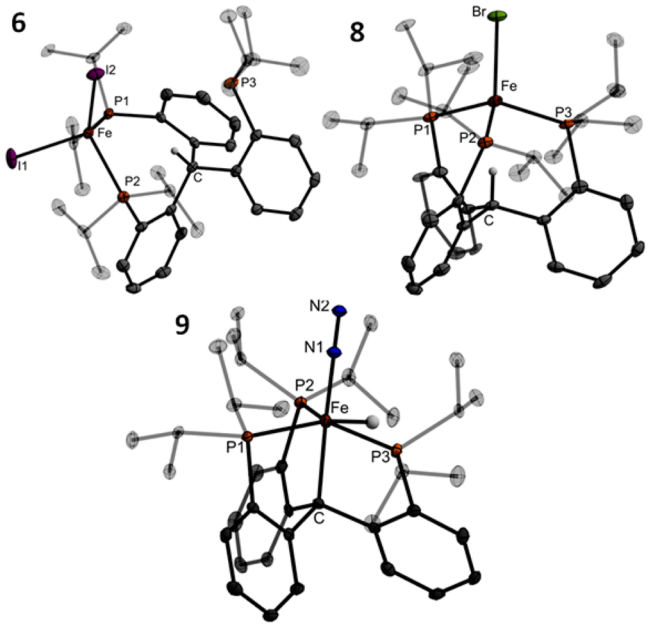

Figure 3. Crystal structures of $\{(CP^{iPr}_3)H\}FeI_2$ (**6**, top left), $\{(CP^{iPr}_3)H\}$FeBr (**8**, top right), and $(CP^{iPr}_3)Fe(H)(N_2)$ (**9**, bottom). Ellipsoids shown at 50% probability; hydrogen atoms (except the triarylmethine C−H and Fe−H hydride) and solvent molecules omitted for clarity.

electron reduction of **6** in benzene or toluene using a range of reagents including sodium amalgam, potassium graphite, or alkylmagnesium/lithium reagents, results in the formation of the deep brick-red four-coordinate iron(I) complex $\{(CP^{iPr}_3)$-$H\}$FeI (**7**). The bromide congener, $\{(CP^{iPr}_3)H\}$FeBr (**8**), is analogously prepared and has been crystallographically characterized (Figure 3); its most notable feature is the endo orientation of the unactivated methine C−*H*. This proton is located within the ligand cage pointed nearly linearly toward the iron center. Both **7** and **8** are unstable with respect to disproportionation to Fe(0), $(CP^{iPr}_3)H$, and $\{(CP^{iPr}_3)H\}FeX_2$ (X = I, Br), especially in coordinating solvents. However, if appropriate conditions are employed, **7** is sufficiently long-lived to be generated and used without further purification for subsequent reactions.

Further reduction of **7** with sodium metal in a 5:1 mixture of Et_2O and DME at −78 °C causes formal insertion of the Fe center into the C−H bond of the $(CP^{iPr}_3)H$ ligand and uptake of atmospheric N_2 to give yellow, diamagnetic $(CP^{iPr}_3)Fe(H)$-(N_2) (**9**). The position of the iron hydride is identifiable in the XRD difference map of **9**, as is the presence of an Fe−C bond at 2.155(2) Å (Figure 3). IR data for **9** show a strong N−N vibration at 2046 cm^{-1} and an Fe−H vibration at 1920 cm^{-1}. The properties of **9** can be compared to the isostructural $(SiP^{iPr}_3)Fe(H)(N_2)$ and $[(NP^{iPr}_3)Fe(H)(N_2)]^+$ complexes[23,33] and other closely related species such as $\{[P(CH_2CH_2P^iPr_2)_3]$-$Fe(H)(N_2)\}^+$;[34] the vibrational and metrical properties of the N_2 ligand suggest a more activated dinitrogen moiety in **9** relative to its congeners.

Deprotonation of **9** to afford $(CP^{iPr}_3)FeN_2^-$ was canvassed but proved unsuccessful. A more circuitous but ultimately effective route to $(CP^{iPr}_3)FeN_2^-$ proceeded via treatment of **9**

dx.doi.org/10.1021/ja4114962 | J. Am. Chem. Soc. XXXX, XXX, XXX−XXX

with anhydrous HCl in Et_2O to afford dark red-orange $(CP^{iPr}_3)FeCl$ (**10**) in good yield (Scheme 2). The crystal structure of **10** was not reliably determined due to its propensity to crystallize in a cubic space group with extensive whole molecule disorder. Complex **10** is paramagnetic and its room temperature solution magnetic moment of 4.9 μ_B is suggestive of a high-spin, $S = 2$ ground state. A lower spin state might have been reasonably anticipated to arise from a presumably strong-field ligand set composed of three diisopropylarylphosphines and an alkyl group. For comparison, $(SiP^{iPr})_3FeCl$ exhibits an intermediate $S = 1$ ground state.[24] The C_{alkyl} anchor in **10** thereby appears to be a weaker-field donor than the silyl anchor in $(SiP^{iPr})_3FeCl$.

Synthesis and Characterization of the $\{(CP^{iPr}_3)FeN_2\}^n$ ($n = 0, -1, +1$) Series. Reduction of the chloride precursor **10** affords entry into the desired series of trigonal bipyramidal iron dinitrogen complexes. Stirring **10** over sodium metal in THF produces the neutral low-spin Fe(I) complex $(CP^{iPr}_3)FeN_2$ (**11**) (υ(NN) = 1992 cm^{-1}) (Scheme 3). Complex **11** is low-spin and paramagnetic ($S = 1/2$); it has been crystallographically characterized (Figure 4) and shows a distortion from trigonal symmetry with one widened P–Fe–P angle (132.5°), as expected due to the Jahn–Teller active ground state. The N_2 vibrational frequency and N–N bond length (1.134(4) Å) show that the dinitrogen ligand in this complex is somewhat more activated than that in the isoelectronic $(SiP^{iPr}_3)FeN_2$ complex (υ(NN) = 2003 cm^{-1}, N–*N* = 1.1245(2) Å) or in the neutral Fe(0) complex $(TP^{iPr}B)FeN_2$ (υ(NN) = 2011 cm^{-1}).[17,25] These differences are relatively small and as such are difficult to reliably interpret. But given the fact that (CP^{iPr}_3) appears to have a weaker-field donor set than (SiP^{iPr}_3) according to the observed ground spin states of $(CP^{iPr}_3)FeCl$ ($S = 2$) and $(SiP^{iPr}_3)FeCl$ ($S = 1$), one might have reasonably anticipated $(SiP^{iPr}_3)FeN_2$ to have a lower υ(NN) than $(CP^{iPr}_3)FeN_2$.

Both a one-electron oxidation and a one-electron reduction of **11** are accessible (Figure 5). The Fe(II/I) couple appears at −1.20 V (vs Fc/Fc^+) and is quasi-reversible; the current in the cathodic wave is diminished and an irreversible reduction wave appears at −1.65 V. This is very similar electrochemical behavior to what has been documented for $(SiP^{iPr}_3)FeN_2$ and suggests that the same phenomenon is responsible for the observations in this system[17]—that is, N_2 coordinates reversibly to the $\{(CP^{iPr}_3)Fe\}^+$ complex; partial loss of N_2 upon oxidation of $(CP^{iPr}_3)FeN_2$ is likely responsible for the quasi-reversibility of the (II/I) couple, and the reduction at −1.65 V is most reasonably attributed to the cationic species $\{(CP^{iPr}_3)Fe(L)\}^+$ (where L may be THF, or may be a vacant site), which then takes up N_2 upon reduction. The Fe(I/0) couple is fully reversible, consistent with the formation of a stable (CP^{iPr}_3)-FeN_2^- anion. This reduction occurs at an unusually negative

Scheme 3. Synthesis of the Dinitrogen Adduct Series $(CP^{iPr}_3)FeN_2$ (11), $(CP^{iPr}_3)FeN_2^-$ (12), and $(CP^{iPr}_3)FeN_2^+$ (13)

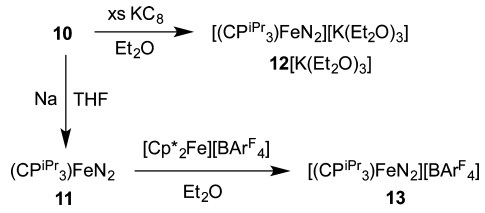

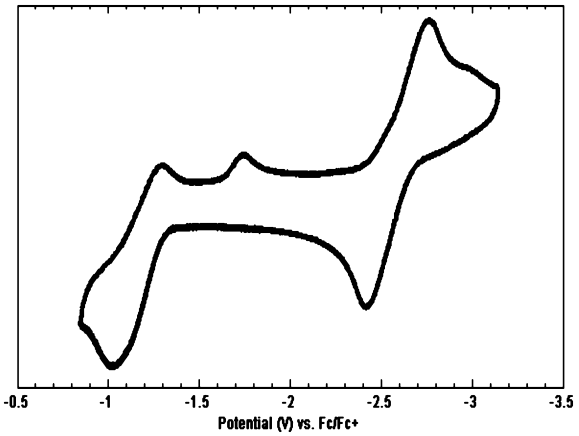

Figure 5. Cyclic voltammogram of **11**; scan rate 0.5 V/s.

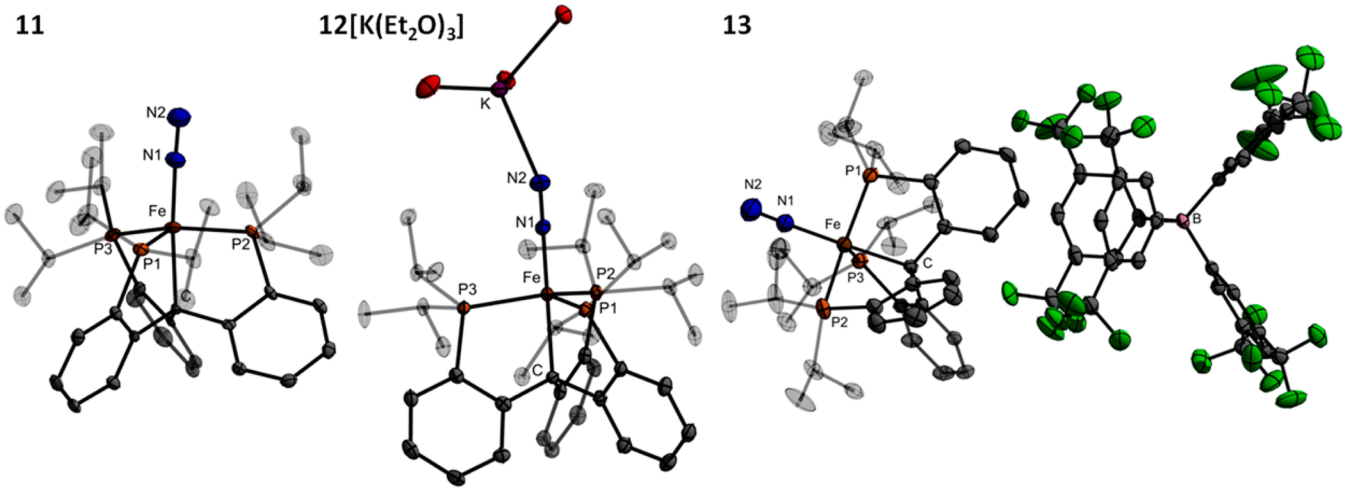

Figure 4. Crystal structures of $(CP^{iPr}_3)FeN_2$ (**11**, left), $(CP^{iPr}_3)FeN_2^-$ (**12**$[K(Et_2O)_3]$, center, ethyl groups of coordinated Et_2O molecules omitted), and $(CP^{iPr}_3)FeN_2^+$ (13, right). Ellipsoids are shown at 50% probability and hydrogen atoms are omitted for clarity.

dx.doi.org/10.1021/ja4114962 | J. Am. Chem. Soc. XXXX, XXX, XXX–XXX

potential (−2.55 V vs Fc/Fc^+). For comparison, the reduction of $(SiP^{iPr}_3)FeN_2$ to $(SiP^{iPr}_3)FeN_2^-$ occurs at −2.2 V.[17]

The Fe−N_2 adduct triad $\{(CP^{iPr}_3)FeN_2\}^n$ (n = 0 (**11**), −1 (**12**), +1 (**13**)) proved synthetically accessible. Treatment of **10** with an excess of potassium graphite (KC_8) in Et_2O results in immediate reduction to the very dark brown-blue $CP^{iPr}_3FeN_2^-$ anion (**12**). The IR spectrum of a thin film deposited from diethyl ether solution shows a υ(NN) vibration at 1870 cm^{-1}, suggestive of a close ion pair with the potassium ion capping the N_2 moiety. Accordingly, treatment of the potassium complex with two equivalents of 12-crown-4 results in the formation of $[(CP^{iPr}_3)FeN_2][K(12\text{-crown-}4)_2]$ (**12**[K(12-crown-4)$_2$]) with a shift of the υ(NN) vibration to 1905 cm^{-1}. The anion has been crystallographically characterized (Figure 4) as its $K(Et_2O)_3$ salt, $[(CP^{iPr}_3)FeN_2][K(Et_2O)_3]$ (**12**[$K(Et_2O)_3$]; the bulk material after drying is solvated by 0.5 molecules of Et_2O per anion, **12**[$K(Et_2O)_{0.5}$]).

Oxidation of **11** with 1 equiv of $[Cp^*_2Fe][BAr^F_4]$ (Ar^F = 3,5-trifluoromethylphenyl; Cp* = pentamethylcyclopentadienide) in Et_2O gives rise to $[(CP^{iPr}_3)FeN_2][BAr^F_4]$ (**13**) as an orange crystalline solid, which has also been structurally characterized (Figure 4). The dinitrogen ligand in **13** (υ(NN) = 2128 cm^{-1}), is labile and in solution under an N_2 atmosphere appears to be in equilibrium with a solvated or vacant cation $[(CP^{iPr}_3)Fe(L)]^+$; in addition to the electrochemical properties discussed above, evidence from UV−vis spectroscopy is consistent with the loss of coordinated N_2 under vacuum (see Supporting Information, SI).

Whereas a related series was accessible for the silyl-anchored $\{(SiP^{iPr}_3)FeN_2\}^n$ system (n = 0, +1, −1),[17] only the anion $(C^{Si}P^{Ph}_3)FeN_2^-$ proved accessible for the previously reported C_{alkyl}-anchored system.[22] Hence, the present $\{(CP^{iPr}_3)FeN_2\}^n$ series allows for a direct comparison of how the anchoring atom (Si vs C) responds across three redox states when positioned trans to an N_2 ligand of an isostructural trigonal bipyramidal framework.

In the case of the $\{(SiP^{iPr}_3)FeN_2\}^n$ series, the Fe−Si bond distance *decreases* upon reduction from 2.298(7) Å in the $(SiP^{iPr}_3)FeN_2^+$ cation to 2.2526(9) Å in the $(SiP^{iPr}_3)FeN_2^-$ anion (Table 1). In direct contrast, the Fe−C bond distance in $\{(CP^{iPr}_3)FeN_2\}^n$ *increases* upon reduction, from 2.081(3) Å in **13** to 2.152(3) Å in **11** to 2.1646(17) Å in **12**. The different responses manifest in these two systems may be due to the electropositive silicon atom binding more strongly to the more electron-rich iron, whereas the more electronegative C_{alkyl} binds more strongly to the higher-valent, more electron-deficient iron center.

Table 1. Select Characterization Data for the Fe−N_2 Adducts $\{(CP^{iPr})_3FeN_2\}^n$ and $\{(SiP^{iPr}_3)FeN_2\}^n$ (n = −1, 0, 1)

X = C, Si[a]	$[X-Fe-N_2]^{-b}$	X−Fe−N_2	$[X-Fe-N_2]^+$
Fe−C (Å)	2.1646(17)	2.152(3)	2.081(3)
Fe−Si (Å)	2.2526(9)	2.2713(6)	2.298(7)
$Fe-N_{X=C}$ (Å)	1.7397(16)	1.797(2)	1.864(7)
$Fe-N_{X=Si}$ (Å)	1.763(3)	1.8191(1)	1.914(2)
$\nu(N_2)_{X=C}$ (cm^{-1})	1870	1992	2128
$\nu(N_2)_{X=Si}$ (cm^{-1})	1891	2003	2143
spin state	S = 0	S = 1/2	S = 1

[a]All data tabulated for X = Si is taken from ref 17. [b]For X = C, data provided is for the $[K(Et_2O)_3]^+$ salt (Figure 4). For X = Si, data provided is for the $[Na(THF)_3]^+$ salt.

Notably, the overall change in the bond length is greater in the CP^{iPr}_3 case (0.084 Å from **13** to **12**) than for the more covalent SiP^{iPr}_3 system, where the overall change is only 0.045 Å despite the longer total bond length. This suggests a greater degree of flexibility in the Fe−C_{alkyl} interaction. A similar conclusion was drawn for the $\{(C^{Si}P^{Ph}_3)Fe(CO)\}^n$ (n = +1, 0, −1) series, where an even more pronounced Fe−C lengthening was observed upon reduction.[22]

In the case of the $(TP^{iPr}B)Fe$ system, a highly flexible Fe−B interaction has been observed as a function of the ligand positioned trans to the B-atom that may be important to its success in activating N_2 in both stoichiometric and catalytic reactions.[15,21,35] However, an analogous series of N_2 complexes has not been characterized to allow for direct comparison. Whereas the anion $[(TP^{iPr}B)]FeN_2]^-$ has been studied by X-ray crystallography (Fe−B = 2.311(2) Å), the $[(TP^{iPr}B)Fe]^+$ cation does not coordinate N_2 at atmospheric pressure, and attempts to obtain the crystal structure of neutral $(TP^{iPr}B)FeN_2$ have been unsuccessful.[25,35] Nonetheless, our chemical intuition is that the Fe−B linkage in $(TP^{iPr}B)Fe$ will be appreciably more flexible than the Fe−C linkage in $(CP^{iPr}_3)Fe$.

The C_{alkyl}-Fe interactions in both $(CP^{iPr}_3)FeN_2^-$ (**12**) and $(C^{Si}P^{Ph}_3)FeN_2^-$ reflect a higher degree of ionic character than in a prototypical Fe−C_{alkyl} bond, with $(C^{Si}P^{Ph}_3)FeN_2^-$ being most striking in this context.[22] Comparative DFT studies of $(C^{Si}P^{Ph}_3)FeN_2^-$ and $(CP^{iPr}_3)FeN_2^-$ including NBO analyses, support this view,[22,36] predicting strong polarization of the σ-bond pair toward the C-atom (23% Fe/77% C in $(C^{Si}P^{Ph}_3)FeN_2^-$; 27% Fe/73% C in $(CP^{iPr}_3)FeN_2^-$) (Figure 6). As expected, the Fe−C bond in **12** is slightly more covalent than that in $(C^{Si}P^{Ph}_3)FeN_2^-$, where the axial carbon is flanked by electropositive silicon atoms. Comparative NBO analyses for $(C^{Si}P^{Ph}_3)FeN_2^-$, $(SiP^{iPr}_3)FeN_2^-$, and simplified model systems were discussed at greater length in a previous report.[22]

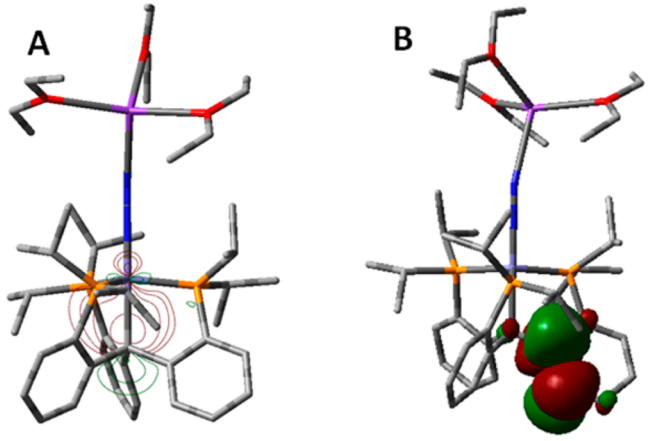

Figure 6. (A) Isocontour plot of the Fe−C_{alkyl} σ bond of **12**[$K(Et_2O)_3$] located from NBO analyses. (B) Contour plot of one of the C_{aryl} π^* orbitals which accepts delocalized electron density from the Fe−C_{alkyl} σ bond.

Second-order perturbation analysis from an NBO calculation indicates the presence of stabilizing donor−acceptor interactions between filled and virtual orbitals, representing deviations from a simple Lewis structure description due to electronic delocalization.[36] In the case of **12**, significant interactions between the filled Fe−C_{alkyl} σ bond and π^* orbitals of the aryl rings ($C_{ipso}-C_{ortho}$) are evident (Figure 6).

dx.doi.org/10.1021/ja4114962 | J. Am. Chem. Soc. XXXX, XXX, XXX−XXX

Three primary donor−acceptor interactions (one to each ring) are located, representing stabilizations of 6.70 kcal/mol, 5.99 kcal/mol, and 5.95 kcal/mol. This result suggests that stabilization of the negative charge on carbon by delocalization onto the aryl rings is at least partially responsible for the observed ionic character of the Fe−C bond, and hence for its increased flexibility. We suggest that a similar stabilization of ionic character at an N_2−Fe−$C_{interstitial}$ site of the cofactor may facilitate N_2 binding.

Reactivity Studies. To compare the reactivity of $(CP^{iPr}_3)FeN_2^-$ at the bound N_2 ligand with $(SiP^{iPr}_3)FeN_2^-$, $(C^{Si}P^{Ph}_3)FeN_2^-$, and $(TP^{iPr}B)FeN_2^-$, treatment of **12** with TMSCl at −78 °C was examined and afforded the diamagnetic diazenido complex $(CP^{iPr}_3)FeN_2SiMe_3$ (**14**) (υ(NN) = 1736 cm^{-1}). This product, although not structurally characterized, is spectroscopically similar to complexes of the structurally related Si- and B-anchored systems.[15,17]

More interesting is the comparative behavior of $(CP^{iPr}_3)FeN_2^-$ on treatment with proton/electron equivalents at low temperature. Numerous studies have explored the possibility of Fe−N_2 protonation/reduction to release ammonia,[3−6,37] which in all but one case[21] afforded low chemical yields of NH_3 (ca. ≤ 10% per Fe in one step; 35% per Fe overall in two independent synthetic steps[14]). The previously described C-anchored system $(C^{Si}P^{Ph}_3)FeN_2^-$ (Figure 2) followed a similar trend, affording negligible NH_3 on treatment at low temperature with $[H(Et_2O)_2][BAr^F_4]$ and KC_8. The Si-anchored system $(SiP^{iPr}_3)FeN_2^-$ also afforded substoichiometric NH_3 yields (35% per Fe) when similarly treated, and instead produced some N_2H_4 (~45% per Fe) when $H(Et_2O)BF_4$ and $CrCl_2$ were employed.[24]

By contrast, cooling a solution of **12**$[K(Et_2O)_{0.5}]$ in Et_2O at −78 °C followed by the addition of 40 equiv KC_8 and then 38 equiv $[H(Et_2O)_2][BAr^F_4]$ leads to the formation of 4.6 ± 0.8 equiv NH_3 (230% per Fe; average of 8 runs; eq 1), a yield that establishes a modest degree of N_2 reduction catalysis at low temperature. No N_2H_4 is observed. With **12**$[K(12\text{-crown-}4)_2]$ as the catalyst, the NH_3 yield is slightly lower at 3.5 ± 0.3 equiv. NH_3 quantification was carried out by UV−vis using the indophenol protocol[38] as recently described in detail for the $(TP^{iPr}B)FeN_2^-$ catalyst system.[21] The total NH_3 product yield is lower for $(CP^{iPr}_3)FeN_2^-$ than that which was obtained for $(TP^{iPr}B)FeN_2^-$ when acid was added prior to the reductant. The significance of these modest differences is unclear, especially given the extreme air-sensitivity of the catalysts and the low turnover numbers. The order of addition of reagents has a minor effect; reversing the order and adding first acid, then reductant to **12**$[K(Et_2O)_{0.5}]$ decreases the yield to 3.8 ± 0.6 equiv NH_3 per Fe. In side-by-side comparisons using the same batches of reagents (KC_8 and $[H(Et_2O)_2][BAr^F_4]$) and the same order of addition (*reductant added first*), **12**$[K(Et_2O)_{0.5}]$ afforded 4.4 ± 0.2 equiv NH_3 per Fe, as compared to 5.0 ± 1.1 for $(TP^{iPr}B)FeN_2^-$ and 0.8 ± 0.4 for $(SiP^{iPr}_3)FeN_2^-$.

$$\begin{array}{c} N_2\ (1\ atm) \\ + \\ xs\ KC_8 \\ + \\ xs\ HBAr^F_4{\cdot}2\ (Et_2O) \end{array} \xrightarrow[-78\ ^\circ C, Et_2O]{\mathbf{12}} NH_3\ (4.6\ equiv) \qquad (1)$$

Treatment of **12**$[K(Et_2O)_{0.5}]$ with 10 equiv of $[H(Et_2O)_2][BAr^F_4]$ in the absence of added reductant generates negligible ammonia (<0.05 equiv), implying that both acid and reductant are necessary for the production of substantial amounts of NH_3.

In order to examine possible reasons for the limited turnover for ammonia production with this system, we sought to determine the fate of the precatalyst over the course of the experiment. An analysis of the iron-containing products of a reaction mixture using 10 equiv of $[H(Et_2O)_2][BAr^F_4]$ and 12 equiv of KC_8 (Figure 7) identified the major iron-containing

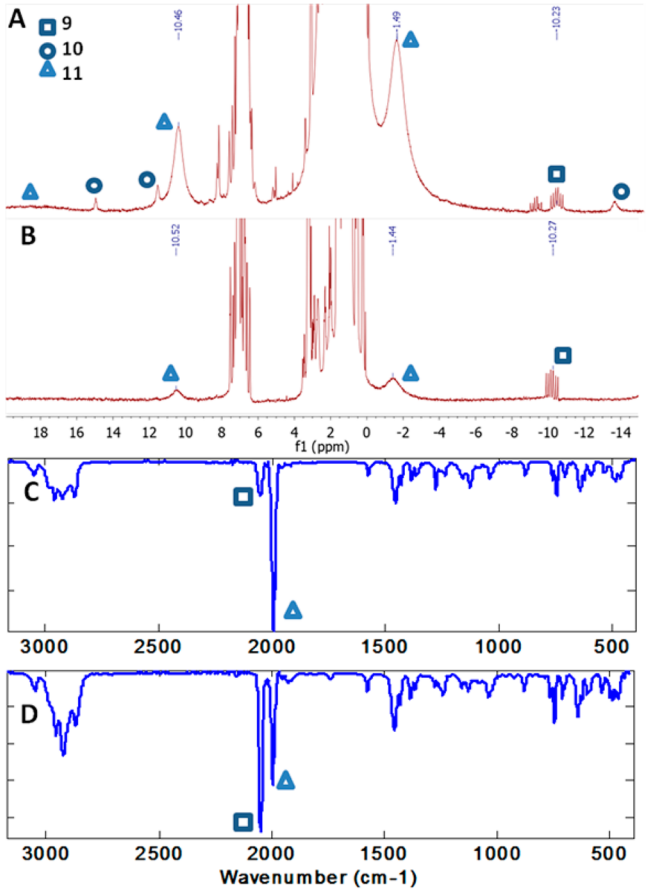

Figure 7. Spectroscopic analyses of reaction mixtures following the catalytic production of NH_3 using **12**$[K(Et_2O)_{0.5}]$ as a catalyst. Symbols indicate characteristic resonances attributed to **9**, **10**, and **11**. (A),(C) ^{1}H NMR and IR spectra of a postcatalytic reaction mixture using 10 equiv of $[H(Et_2O)_2][BAr^F_4]$ and 12 equiv of KC_8. (B),(D) ^{1}H NMR and IR spectra of a postcatalytic reaction mixture using 38 equiv of $[H(Et_2O)_2][BAr^F_4]$ and 40 equiv of KC_8.

product as $(CP^{iPr}_3)FeN_2$ (**11**), which is readily reduced by KC_8 even at low temperature to reform the precatalyst **12**. However, a significant amount of $(CP^{iPr}_3)Fe(N_2)(H)$ (**9**) is also present; **9** is not catalytically competent, generating no detectable ammonia when subjected to the catalytic conditions, and its formation is likely an important limiting factor in the catalyst performance. Another identifiable species by ^{1}H NMR spectroscopy is $(CP^{iPr}_3)FeCl$ (**10**). Despite our efforts to remove all Cl^- in the preparation of $[H(Et_2O)_2][BAr^F_4]$, the large excess of acid employed in this experiment likely ensures a non-negligible Cl^- impurity that may also attenuate catalyst activity. The identity of another diamagnetic hydride-bearing

dx.doi.org/10.1021/ja4114962 | J. Am. Chem. Soc. XXXX, XXX, XXX−XXX

species apparent in the ^{1}H NMR spectrum is not currently known.

Further product analysis using the full catalytic conditions (38 equiv of $[H(Et_2O)_2][BAr^F{}_4]$ and 40 equiv of KC_8 with respect to the catalyst), showed that increasing amounts of $(CP^{iPr}{}_3)Fe(N_2)(H)$ (**9**) are formed as the system turns over, corroborating the idea that this species serves as a catalytically inactive sink which builds up throughout the reaction. Integration of the NMR spectrum of such a reaction mixture against an internal standard suggests that approximately 70% of the catalyst has been converted to **9** (see SI); even at this point, however, some active catalyst remains in the form of **11** (Figure 7). The unknown hydride species present in the aforementioned reaction mixture, derived from fewer equivalents of acid and reductant, is no longer observed.

Notably, in neither of these experiments is any free ligand **1** (nor any ligand decomposition product) detected; it appears that all of the iron present remains ligated by the $CP^{iPr}{}_3$ ligand. This lack of degradation is promising, and suggests that improvements to the N_2 reduction catalysis, in terms of turnover number, may yet prove possible if the formation of terminal hydride **9** can be limited by modification of either the ligand scaffold and/or the catalytic conditions. Indeed, it may be that biological nitrogenases are designed to avoid catalytically inactive hydride sinks by evolving hydrogen.[39] An iron-sulfur cluster might be a particularly good design in this context.[40]

CONCLUSIONS

To conclude, we have synthetically introduced the tripodal $(CP^{iPr}{}_3)H$ ligand and have prepared and structurally compared its $\{(CP^{iPr}{}_3)FeN_2\}^n$ complexes ($n = 0, -1, +1$) with those of the isostructural series $\{(SiP^{iPr}{}_3)FeN_2\}^n$. The $\{(CP^{iPr}{}_3)FeN_2\}^n$ complexes feature an axial N_2 ligand bound trans to an axial C-atom in a trigonal bipyramidal geometry, a design meant to crudely model one plausible geometry for a single Fe−N_2 binding site in the iron−molybdenum cofactor (FeMoco). The C_{alkyl}−Fe interaction in the $(CP^{iPr}{}_3)Fe$ system exhibits a substantially higher degree of ionic character, and is more flexible, than for the related Si_{silyl}−Fe interaction in the isostructural and isoelectronic $(SiP^{iPr}{}_3)Fe$ system.[17] We suggest that this type of Fe−C flexibility crudely models the flexibility one can intuit for an N_2−Fe−$C_{interstitial}$ interaction within FeMoco. Whereas the N_2 anion $(SiP^{iPr}{}_3)FeN_2^-$ does not effectively facilitate the delivery of H-atoms to N_2 to produce NH_3 via proton/reductant equivalents, an Et_2O solution of isoelectronic and isostructural $(CP^{iPr}{}_3)FeN_2^-$ under 1 atm of N_2 releases ca. 4.6 equiv NH_3 relative to Fe. The modest catalytic N_2 reduction behavior of $(CP^{iPr}{}_3)FeN_2^-$ at −78 °C is comparable to $(TP^{iPr}B)FeN_2^-$.[21]

It is noteworthy that among the isostructural $SiP^{iPr}{}_3$, $TP^{iPr}B$, and $CP^{iPr}{}_3$ series, the system with the most flexible axial linkage, $(TP^{iPr}B)Fe$, gives the greatest catalytic yield under a common set of reaction conditions, while the least flexible, $(SiP^{iPr}{}_3)Fe$, gives only substoichiometric yields of ammonia; the $(CP^{iPr}{}_3)Fe$ system falls in between the two both in terms of flexibility and catalytic competence. While we emphasize caution in interpreting these differences given the low overall turnover numbers, they are consistent with the previously advanced hypothesis that a flexible Fe−$C_{interstitial}$ interaction might facilitate N_2 binding and reduction at a single Fe site. Our structural and DFT studies[22] demonstrate that, in the right environment, a carbon atom can serve as a modestly flexible ligand trans to an Fe−N_2 binding site, and that this flexibility is enhanced by the ability of the carbon to accommodate a significant ionic charge. It seems plausible to us that the inorganic carbide ligand in FeMoco could be similarly, and perhaps more, able to stabilize substantial ionic character in an Fe−$C_{interstitial}$ bond (Figure 1), resulting in a flexible interaction exposing an N_2 binding site that can be further modulated as a function of the N_xH_y reduction state.

At this early stage, reliable conclusions concerning the influence of the carbon atom on the intimate stepwise mechanism of nitrogen reduction are premature. Even within our synthetic series, it may be that different catalysts follow different mechanistic pathways (distal vs alternating, or some hybrid path);[21,41] for instance the most flexible system, $(TP^{iPr}B)Fe$, may be better suited to facilitate a distal pathway that samples strongly π-bonded intermediates, while $(CP^{iPr}{}_3)$-Fe, which we presume is less flexible, could instead be dominated by an alternating or hybrid pathway. Whether these structurally related iron systems mediate nitrogen reduction by a common or different mechanism will be challenging to determine but is a fascinating question. The work presented here adds to the context needed for further mechanistic studies on both synthetic and biological iron systems for catalytic nitrogen fixation.

EXPERIMENTAL METHODS

General. All manipulations were carried out using standard Schlenk or glovebox techniques under an N_2 atmosphere. Unless otherwise noted, solvents were deoxygenated and dried by thoroughly sparging with N_2 followed by passage through an activated alumina column in a solvent purification system by SG Water, USA LLC. Nonhalogenated solvents were tested with a standard purple solution of sodium benzophenone ketyl in tetrahydrofuran in order to confirm effective moisture removal. *O*-Iodotriphenylmethane,[28] $H(OEt_2)_2[B(3,5\text{-}(CF_3)_2\text{−}C_6H_3)_4]$,[42] KC_8,[43] $[(TPB)FeN_2][Na(12\text{-crown-}4)_2]$,[25] $[(SiP^{iPr}{}_3)FeN_2][Na(12\text{-crown-}4)_2]$[17] and $[(C^{Si}P^{Ph}{}_3)FeN_2][K(18\text{-crown-}6)_2]$[22] were prepared according to literature procedures. [Decamethylferrocenium][$B(3,5\text{-}(CF_3)_2\text{-}C_6H_3)_4$] was prepared by treating [ferrocenium][$B(3,5\text{-}(CF_3)_2\text{−}C_6H_3)_4$][44] with decamethylferrocene and used without purification. $FeI_2(THF)_2$ was prepared by treating Fe powder with I_2 in THF,[45] and was dried to FeI_2 by heating under vacuum at 80 °C for 6 h. All other reagents were purchased from commercial vendors and used without further purification unless otherwise stated.

Physical Methods. Elemental analyses were performed by Robinson Microlit Laboratories (Ledgewood, NJ). Deuterated solvents were purchased from Cambridge Isotope Laboratories, Inc., degassed, and dried over active 3-Å molecular sieves prior to use. ^{1}H and ^{13}C chemical shifts are reported in ppm relative to tetramethylsilane, using residual proton and ^{13}C resonances from solvent as internal standards. ^{31}P and ^{19}F chemical shifts are reported in ppm relative to 85% aqueous H_3PO_4 and $CFCl_3$, respectively. Solution phase magnetic measurements were performed by the method of Evans.[46] Optical spectroscopy measurements were taken on a Cary 50 UV−vis spectrophotometer using a 1-cm two-window quartz cell. Electrochemical measurements were carried out in a glovebox under a dinitrogen atmosphere in a one compartment cell using a CH Instruments 600B electrochemical analyzer. A glassy carbon electrode was used as the working electrode and platinum wire was used as the auxiliary electrode. The reference electrode was Ag/$AgNO_3$ in THF. The ferrocene couple Fc^+/Fc was used as an internal reference. Solutions (THF) of electrolyte (0.2 M tetra-*n*-butylammonium hexafluorophosphate) and analyte were also prepared under an inert atmosphere.

X-ray Crystallography. XRD studies were carried out at the Beckman Institute Crystallography Facility on a Bruker Kappa Apex II diffractometer (Mo Kα radiation). Structures were solved using

dx.doi.org/10.1021/ja4114962 | J. Am. Chem. Soc. XXXX, XXX, XXX−XXX

SHELXS and refined against F^2 on all data by full-matrix least-squares with SHELXL.[47] The crystals were mounted on a wire loop. Methyl group hydrogen atoms not involved in disorder were placed at calculated positions starting from the point of maximum electron density. All other hydrogen atoms, except where otherwise noted, were placed at geometrically calculated positions and refined using a riding model. The isotropic displacement parameters of the hydrogen atoms were fixed at 1.2 (1.5 for methyl groups) times the U_{eq} of the atoms to which they are bonded. Further details for each structure can be found in the SI.

Computations. A single-point calculation and Natural Bond Orbital (NBO) analysis was carried out on $[(CP^{iPr}_3)FeN_2][K(Et_2O)_3]$ (**12**) using the crystallographically determined atomic coordinates at the B3LYP/6-31++G(d,p) level of theory using the Gaussion03 suite of programs.[48] NBO analysis located a polarized σ interaction between Fe and the C-atom anchor (C01). Further details of the computational results can be found in the SI.

10-Phenyl-10*H*-dibenzo[*b,e*]iodininium Bromide (2). The procedure for the generation of **2** and **4** (below) was adapted from a reported method for the generation of diaryliodonium salts.[29] 3-Chloroperoxybenzoic acid (9.0 g, ∼70% by mass, ∼0.037 mol) was dissolved in dichloromethane (150 mL) and cooled to 0 °C. 2-Iodotriphenylmethane (11.7 g, 0.0316 mol) was added as a solid in portions over the course of 10 min, during which time there was no observable change to the reaction mixture. This mixture was stirred at 0 °C for 10 min and then neat trifluoromethanesulfonic acid (8.74 mL, 0.0990 mol) was added via syringe over the course of 5 min. The reaction mixture turned dark brown. After an additional 20 min, the reaction mixture was allowed to warm to room temperature and stirred for 1 h, and then the solvent was removed in vacuo. The solid material was suspended in 200 mL of diethyl ether and 200 mL of water, and then solid sodium bromide (14 g, 0.136 mol) was added, and the mixture was shaken vigorously for 5 min, during which time a fine off-white precipitate developed. The precipitate was collected atop a sintered glass frit and washed copiously with water and diethyl ether (14.2 g, 0.0316 mol, quant). ^{1}H NMR ($(CD_3)_2S{=}O$, 300 MHz, 298 K, δ): 8.27 (dd, J = 8 Hz, 1 Hz, 2H), 7.68 (td, J = 8 Hz, 1 Hz, 2H), 7.46 (td, J = 8 Hz, 1 Hz), 7.27 (m, 3H), 6.78 (dm, J = 8 Hz, 2H), 6.09 (s, 1H) ppm. ^{13}C NMR ($(CD_3)_2S{=}O$, 75.4 MHz, 298 K, δ): 140.3 (s), 138.3 (s), 135.0 (s), 132.7 (s), 131.7 (s), 129.6 (s), 128.9 (s), 127.9 (s), 127.4 (s), 117.4 (s), 57.7 (s) ppm. ESI-MS (positive ion, amu): Calcd. 370.0; Found 370.0.

2-Bromo-2′-iodotriphenylmethane (3). 10-Phenyl-10*H*-dibenzo[*b,e*]iodininium bromide (16.11 g, 0.0358 mol) was suspended in dry, degassed acetonitrile (250 mL), and solid tetrabutylammonium bromide (25 g, 0.078 mol) and copper(I) bromide (8 g, 0.06 mol) were added. The mixture was heated to a vigorous reflux and stirred at reflux for five days. The dark brown reaction mixture was then concentrated to dryness in vacuo, extracted with toluene, and filtered through a silica plug. The pale yellow filtrate was concentrated to dryness, and the resulting material was recrystallized from methanol to give the desired product as an off-white powder which was collected atop a sintered glass frit and washed with cold methanol (12.7 g, 0.0282 mol, 79%). ^{1}H NMR ($CDCl_3$, 300 MHz, 298 K, δ): 7.90 (dd, J = 8 Hz, 1 Hz, 1H), 7.60 (dd, J = 8 Hz, 1 Hz, 1H), 7.34−7.18 (m, 5H), 7.13 (td, J = 8 Hz, 1 Hz, 1H), 7.03 (dd, J = 8 Hz, 1 Hz, 2H), 6.95 (td, J = 8 Hz, 1 Hz, 1H), 6.79 (dd, J = 8 Hz, 1 Hz, 2H), 6.02 (s, 1H) ppm. ^{13}C NMR ($CDCl_3$, 75.4 MHz, 298 K, δ): 145.2 (s), 142.2 (s), 141.1 (s), 140.1 (s), 133.1 (s), 131.2 (s), 130.7 (s), 130.0 (s), 128.5 (s), 128.3 (s), 128.2 (s), 128.0 (s), 127.2 (s), 126.7 (s), 126.3 (s), 102.9 (s), 60.8 (s) ppm. MS (amu): Calcd. 449.9, 447.9; Found 449.9, 447.9.

10-(2-Bromophenyl)-10*H*-dibenzo[*b,e*]iodininium Iodide (4). 3-Chloroperoxybenzoic acid (5 g, ∼70% by mass, ∼0.0203 mol) was dissolved in dichloromethane (200 mL) and cooled to 0 °C. 2-Bromo-2′-iodotriphenylmethane (8.2 g, 0.0182 mol) was added as a solid in portions over the course of 10 min, during which time there was no observable change in the reaction mixture. This mixture was stirred at 0 °C for 10 min and then neat trifluoromethanesulfonic acid (5.04 mL, 0.0571 mol) was added via syringe over the course of 5 min. The reaction mixture turned dark brown. After an additional 30 min, the reaction mixture was allowed to warm to room temperature and stirred for 30 min, and then the solvent was removed in vacuo. The solid material was suspended in 200 mL of diethyl ether and 200 mL of water, and then solid potassium iodide (15 g, 0.090 mol) was added and the mixture was shaken vigorously for 5 min, during which time a fine yellow precipitate developed. The precipitate was collected atop a sintered glass frit and washed copiously with water and diethyl ether (9.95 g, 0.0173 mol, 95%). ^{1}H NMR ($(CD_3)_2S{=}O$, 300 MHz, 298 K, δ): 8.20 (dd, J = 8 Hz, 1 Hz, 2H), 7.83 (dd, J = 8 Hz, 1 Hz, 2H), 7.72 (dd, J = 8 Hz, 1 Hz, 1H), 7.60 (td, J = 8 Hz, 1 Hz, 2H), 7.47−7.39 (m, 3H), 7.33 (td, J = 8 Hz, 1 Hz, 1H), 7.23 (dd, J = 8 Hz, 1 Hz, 1H), 6.02 (s, 1H) ppm. ^{13}C NMR ($(CD_3)_2S{=}O$, 75.4 MHz, 298 K, δ): 138.9 (s), 135.4 (s), 135.1 (s), 135.0 (s), 133.4 (s), 132.8 (s), 131.7 (s), 130.7 (s), 130.0 (s), 128.0 (s), 117.2 (s), 110.0 (s), 58.8 (s) ppm. ESI-MS (positive ion, amu): Calcd. 446.9, 448.9; Found 446.9, 448.9.

2-Bromo-2′,2″-diiodotriphenylmethane (5). Solid 10-(2-bromophenyl)-10*H*-dibenzo[*b,e*]iodininium iodide (4.54 g, 7.88 mmol) was sealed inside a Schlenk tube under N_2 and heated to 200 °C for 15 min, and then cooled to room temperature. The resulting dark violet residue was taken up in dichloromethane (50 mL) and washed with saturated aqueous sodium thiosulfate (50 mL) and then water (30 mL) and saturated aqueous sodium chloride (30 mL), then dried over magnesium sulfate, filtered, and concentrated to dryness in vacuo. The resulting off-white residue was recrystallized from methanol to give the desired product as a fine white powder, which was collected atop a sintered glass frit and washed with cold methanol (3.4 g, 5.90 mmol, 75%). ^{1}H NMR ($CDCl_3$, 300 MHz, 298 K, δ): 7.93 (d, J = 8 Hz, 2H), 7.64 (d, J = 8 Hz, 1H), 7.30−7.16 (m, 4H), 7.00 (t, J = 8 Hz, 2H), 6.72 (d, J = 8 Hz, 3H), 6.04 (s, 1H) ppm. ^{13}C NMR ($CDCl_3$, 75.4 MHz, 298 K, δ): 144.1 (s), 141.1 (s), 140.2 (s), 133.3 (s), 131.1 (s), 130.7 (s), 128.6 (s), 128.5 (s), 127.3 (s), 126.7 (s), 103.6 (s), 65.4 (s) ppm. MS (amu): Calcd. 573.8, 575.8; Found 446.9, 448.9 ([M−I]+), 368.1 ([M−I−Br]$^+$), 320.1, 322.1 ([M−2I]$^+$).

Tris(2-(diisopropylphosphino)phenyl)methane ("($C^{iPr}P_3$)H") (1). 2-Bromo-2′,2″-diiodotriphenylmethane (2.00 g, 3.48 mmol) was dissolved in diethyl ether (100 mL) and cooled to −78 °C while stirring. Solid *t*-butyllithium (1.36 g, 21.23 mmol) was added in portions over the course of 10 min, and the reaction mixture was stirred at low temperature for 3 h. Then chlorodiisopropylphosphine (1.96 g, 12.8 mmol) was dissolved in 10 mL of diethyl ether and added to the reaction mixture. The reaction mixture was allowed to warm slowly to room temperature overnight, resulting in the precipitation of a fine white solid. The reaction mixture was filtered through silica and the pale yellow-orange filtrate was concentrated to a sticky yellow solid which was triturated with acetonitrile to give an off-white powder. The solid was washed copiously with acetonitrile and then dried under vacuum, giving 1.4 g (2.36 mmol, 68%) of the desired product. ^{1}H NMR (C_6D_6, 300 MHz, 298 K, δ): 8.15 (q, J = 6 Hz, 1H), 7.44 (d, J = 7 Hz, 3H), 7.06 (td, J = 7 Hz, 2 Hz, 3H), 7.00−6.93 (m, 6H), 2.27 (septet of doublets, J = 4 Hz, 7 Hz, 3H), 1.73 (septet of doublets, J = 3 Hz, 7 Hz, 3H), 1.40 (dd, J = 7 Hz, 13 Hz, 9H), 1.32 (dd, J = 7 Hz, 12 Hz, 9H), 0.88 (dd, J = 7 Hz, 13 Hz, 9H), 0.44 (dd, J = 7 Hz, 12 Hz, 9H) ppm. ^{13}C NMR (C_6D_6, 75.4 MHz, 298 K, δ): 159.0 (d, J = 29 Hz), 144.8 (d, J = 17 Hz), 140.0 (s), 139.3 (s), 132.4 (s), 59.1 (m), 32.7 (m), 30.0 (m), 29.4 (s), 27.3 (m), 21.0 (s) ppm. ^{31}P NMR (C_6D_6, 121.4 MHz, 298 K, δ): −9.1 ppm. Anal. Calcd. for $C_{37}H_{55}P_3$: C, 74.97; H, 9.35. Found: C, 74.73; H, 9.49.

{(CP^{iPr}_3)H}FeI_2 (6). (CP^{iPr}_3)H (500 mg, 0.843 mmol) was added to FeI_2 (350 mg, 1.13 mmol) in 15 mL of toluene and stirred at 60 °C for 2 h, at which point the reaction mixture was filtered through diatomaceous earth and the yellow filtrate was concentrated to give a yellow powder (761 mg, 0.843 mmol, quant). Crystals suitable for X-ray diffraction were grown by layering of pentane over a saturated toluene solution. ^{1}H NMR (C_6D_6, 300 MHz, 298 K, δ): 179.69, 26.00, 18.60, 14.92, 14.28, 13.62, 12.74, 9.96, 9.00, 8.29, 6.76, 6.16, 5.72, 5.48, 4.97, 4.28, 3.78, 0.30, 0.13, −0.48, −0.91, −2.02, −3.68, −5.09, −9.45 ppm. μ_{eff} (C_6D_6, Evans' method, 298 K): 4.85 μ_B.

(CP^{iPr}_3)Fe(N_2)H (9). (CP^{iPr}_3)HFeI_2 (370 mg, 0.410 mmol) was suspended in benzene (10 mL) and stirred vigorously over an excess of 0.7% sodium/mercury amalgam (25 mg Na, 1.1 mmol) for 2 h. The

dx.doi.org/10.1021/ja4114962 | J. Am. Chem. Soc. XXXX, XXX, XXX−XXX

initially yellow suspension turned a deep brick red color during this time due to the formation of {(CP^{iPr}_3)H}FeI (7). The reaction mixture was filtered through diatomaceous earth and concentrated to dryness in vacuo. The deep red residue was then suspended in diethyl ether (15 mL) at −78 °C and 3 mL of dimethoxyethane was added; this solution was vigorously stirred over excess sodium mirror for 4 h at −78 °C, during which time the color lightened to orange. The reaction mixture was then filtered through diatomaceous earth and concentrated to dryness. The residue was extracted into pentane and again filtered through diatomaceous earth, giving a lighter yellow-orange filtrate which was concentrated to dryness again. This residue could be recrystallized from diethyl ether by slow evaporation to give yellow crystalline solids. These solids were washed with hexamethyldisiloxane and minimal cold diethyl ether, and then dried in vacuo to give 155 mg (0.229 mmol, 56%) of the desired product. Crystals suitable for X-ray diffraction were grown by evaporation of a concentrated pentane solution into hexamethyldisiloxane. ^{1}H NMR (C_6D_6, 300 MHz, 298 K, δ): 7.57 (t, J = 6 Hz, 1H), 7.34 (m, 1H), 7.08 (m, 2H), 6.96 (m, 2H), 6.83−6.75 (m, 4H), 6.65 (m, 1H), 6.50 (m, 1H), 2.94 (septet, J = 8 Hz, 1H), 2.75 (m, 2H), 2.36 (septet, J = 6 Hz, 1H), 2.05 (septet, J = 7 Hz, 1H), 1.75−1.17 (m, 25H), 1.02 (dd, J = 7 Hz, 11 Hz, 3H), 0.65 (dd, J = 7 Hz, 15 Hz, 3H), 0.56 (dd, J = 7 Hz, 10 Hz, 3H), 0.27 (dd, J = 8 Hz, 13 Hz, 3H), −10.2 (ddd, J = 38 Hz, 53 Hz, 50 Hz) ppm. ^{31}P NMR (C_6D_6, 121.4 MHz, 298 K, δ): 90.1 (dt, J = 100 Hz, 17 Hz, 1P), 67.0 (m, 1P), 63.4 (dt, J = 100 Hz, 17 Hz, 1P) ppm. IR (thin film; cm^{-1}): 2046 (N−N), 1920 (Fe−H). Anal. Calcd. for $C_{37}H_{55}FeP_3N_2$: C, 65.68; H, 8.19; N, 4.14. Found: C, 65.91; H, 7.89; N, 3.94.

{(CP^{iPr}_3)H}FeBr (8). {(CP^{iPr}_3)H}$FeBr_2$ (5.0 mg, 0.0070 mmol, generated by treating (CP^{iPr}_3)H with anhydrous $FeBr_2$ in toluene) was dissolved in toluene, cooled to −78 °C, and treated with isopropyl magnesium chloride (3.5 μL, 2.0 M in Et_2O). The reaction mixture rapidly turned dark brick-red. It was stirred at low temperature for 1 h and then allowed to warm to room temperature for 30 min before being filtered and concentrated. The dark red powder was not purified, but was analyzed by NMR in C_6D_6, and X-ray quality crystals were grown by layering pentane over a filtered benzene solution.

(CP^{iPr}_3)FeCl (10). (CP^{iPr}_3)Fe(N_2)H (61 mg, 0.0901 mmol) was dissolved in diethyl ether (8 mL) and cooled to −78 °C. HCl in diethyl ether (1.0 M, 108 μL, 0.108 mmol) was added to the solution in one portion. The reaction mixture was stirred at low temperature for 1 h and then warmed to room temperature and stirred overnight. The color darkened to deep red-orange, and the reaction mixture was filtered through diatomaceous earth and concentrated to dryness. The red residue was recrystallized by evaporation of a pentane solution into hexamethyldisiloxane and the resulting dark red crystals were washed sparingly with cold pentane and dried in vacuo, giving 46 mg (0.0673 mmol, 75%) of (CP^{iPr}_3)FeCl. Crystals suitable for X-ray diffraction were grown by evaporation of a concentrated pentane solution into hexamethyldisiloxane. ^{1}H NMR (C_6D_6, 300 MHz, 298 K, δ): 179.93, 26.47, 23.05, 17.44, 17.22, 15.03, 11.66, 1.52, −10.27, −13.36, −16.82 ppm. μ_{eff} (C_6D_6, Evans' method, 298 K): 4.92 μ_B. Anal. Calcd. for $C_{37}H_{54}FeP_3Cl$: C, 65.06; H, 7.97. Found: C, 64.96; H, 8.01.

(CP^{iPr}_3)FeN_2 (11). (CP^{iPr}_3)FeCl (82 mg, 0.120 mmol) was dissolved in THF (2 mL) and stirred over sodium mirror for 20 min, or until NMR analysis showed complete consumption of the starting material, and then filtered and concentrated. The residue was extracted with pentane and filtered through diatomaceous earth, and concentrated to a brownish-orange residue which was recrystallized by evaporation of a pentane solution into hexamethyldisiloxane. The dark brown-orange crystals were washed with hexamethyldisiloxane and cold pentane and dried in vacuo to give 39 mg (0.0581 mmol, 48%) of (CP^{iPr}_3)FeN_2. Crystals suitable for X-ray diffraction were grown by evaporation of a concentrated pentane solution into hexamethyldisiloxane. ^{1}H NMR (C_6D_6, 300 MHz, 298 K, δ): 19.3 (very broad), 10.4, 6.8, 3.0, 2.0, 0.6, −1.4 ppm. μ_{eff} (C_6D_6, Evans' method, 298 K): 1.75 μ_B. IR (thin film; cm^{-1}): 1992 (N−N). Anal. Calcd. for $C_{37}H_{54}FeP_3N_2$: C, 65.78; H, 8.06; N, 4.15. Found: C, 66.03; H, 8.01; N, 3.86.

[(CP^{iPr}_3)FeN_2][$K(Et_2O)_{0.5}$] (12[$K(Et_2O)_{0.5}$]). (CP^{iPr}_3)FeCl (40 mg, 0.0586 mmol) was dissolved in diethyl ether(5 mL) at room temperature and an excess of potassium graphite (KC_8, 25 mg) was added. The reaction mixture was stirred for 10 min and then filtered through diatomaceous earth. The dark brown solution was concentrated to about 2 mL and then pentane was layered over the ether solution, and it was allowed to stand overnight during which time dark bluish-brown crystals formed. The supernatant was decanted, and the crystals were washed thoroughly with pentane and thoroughly dried under vacuum, giving 26 mg of the desired product (0.0277 mmol, 47%). NMR analysis indicates the presence of 0.5 ether solvent molecules per anion. Crystals suitable for X-ray diffraction were grown by vapor diffusion of pentane into a diethyl ether solution; in these crystals the potassium cation is solvated by three diethyl ether molecules. ^{1}H NMR (d_8-THF, 300 MHz, 298 K, δ): 7.04 (s, 3H), 6.67 (s, 3H), 6.47 (s, 6H), 3.38 (q, J = 7 Hz, 2H, diethyl ether ($CH_3CH_2)_2O$), 2.99 (br s, 3H), 2.14 (br s, 3H), 1.42 (d, J = 6 Hz, 9H), 1.36 (d, J = 5 Hz, 9H), 1.12 (t, J = 7 Hz, 3H, diethyl ether ($CH_3CH_2)_2O$), 1.01 (d, J = 5 Hz, 9H), 0.12 (d, 9H) ppm. ^{31}P NMR (5:1 C_6D_6/d_8-THF, 121.4 MHz, 298 K, δ): 68.1 ppm. IR (thin film deposited from Et_2O; cm^{-1}): 1870 (N−N).

[(CP^{iPr}_3)FeN_2][$K(12\text{-c-}4)_2$] (12[$K(12\text{-c-}4)_2$]). A sample of **12** (15 mg, 0.020 mmol) was dissolved in diethyl ether (1 mL) and 12-crown-4 (8.8 mg, 0.050 mmol) was added as a solution in diethyl ether (1 mL). The resulting solution was layered with pentane and allowed to stand overnight, resulting in the crystallization of **12**[$K(12\text{-crown-}4)_2$] as a very dark blue solid. The crystals were washed with pentane and dried under vacuum, giving 10 mg of material (53% yield). ^{1}H NMR (d_8-THF, 300 MHz, 298 K, δ) 6.86 (br s, 6H), 6.47 (s, 6H), 3.62 (s, 36H, 12-crown-4), 1.43 (s, 9H), 1.30 (s, 9H), 0.91 (s, 9H), 0.16 (s, 9H) ppm. ^{31}P (C_6D_6, 121.4 MHz, 298 K, δ): 66 ppm. IR (thin film; cm^{-1}) 1905 (N−N).

[(CP^{iPr}_3)FeN_2][$B(3,5\text{-}(CF_3)_2\text{−}C_6H_3)_4$] (13). ($CP^{iPr}_3$)$FeN_2$ (7.3 mg) was dissolved in diethyl ether (1 mL) and a solution of [$Fe(C_5Me_5)_2$]-[$B(3,5\text{-}(CF_3)_2\text{−}C_6H_3)_4$] in diethyl ether (1 mL) was added dropwise while stirring at room temperature. The reaction mixture was then concentrated to give an orange solid which was washed with benzene and then dried in vacuo. Crystals suitable for X-ray diffraction were grown by slow evaporation of a diethyl ether solution into hexamethyldisiloxane. ^{1}H NMR (4:1 C_6D_6/THF-d_8 under N_2, 300 MHz, 298 K, δ): 16.65, 14.48, 8.15, 7.60, 2.71 ppm. (Note: the exact position of the paramagnetically shifted NMR peaks varies with the composition of the solvent due to the likely exchange of the N_2 ligand with THF). μ_{eff} (d_8-THF, Evans' method, 298 K): 4.3 μ_B. IR (thin film; cm^{-1}): 2128 (N−N). Satisfactory elemental analysis could not be obtained due to the lability of the coordinated N_2 ligand.

(CP^{iPr}_3)FeN_2SiMe_3 (14). [(CP^{iPr}_3)FeN_2][$K(Et_2O)_{0.5}$] (35 mg, 0.0465 mmol) was dissolved in diethyl ether (2 mL) and cooled to −78 °C. Trimethylsilyl chloride (6 μL, 0.0473 mmol) was dissolved in diethyl ether (1 mL) and added dropwise to the stirring reaction mixture. The reaction was stirred at low temperature for one hour and then warmed to room temperature for 1 h, concentrated to dryness, taken up in pentane, filtered through diatomaceous earth, and concentrated. The red-orange residue was recrystallized by slow evaporation of a pentane solution into hexamethyldisiloxane, and the resulting red solids were washed with cold hexamethyldisiloxane and dried in vacuo to give 21 mg (0.0280 mmol, 60%) of solid material, which was contaminated with a small amount of CP_3FeN_2 (**11**) which we were unable to remove by repeated recrystallization. **14** decomposes slowly to **11** over time. ^{1}H NMR (C_6D_6, 300 MHz, 298 K, δ) 7.33 (br m, 3H), 6.80 (t, J = 4 Hz, 6H), 6.63 (m, 3H), 2.67 (septet, J = 7 Hz, 3H), 1.97 (septet, J = 7 Hz, 3H), 1.45 (m, 18H), 0.96 (q, J = 7 Hz, 9H), 0.72 (q, J = 7 Hz, 9H), 0.12 (s, 3H) ppm. ^{31}P (C_6D_6, 121.4 MHz, 298 K, δ): 80.1 ppm. IR (thin film; cm^{-1}) 1736 (N−N).

Ammonia Quantification. A Schlenk tube was charged with HCl (4 mL of a 1.0 M solution in Et_2O, 4 mmol). Reaction mixtures were vacuum transferred into this collection flask. Residual solid in the reaction vessel was treated with a solution of [Na][O-*t*-Bu] (40 mg, 0.4 mmol) in 1,2-dimethoxyethane (1 mL) and sealed. The resulting

dx.doi.org/10.1021/ja4114962 | J. Am. Chem. Soc. XXXX, XXX, XXX−XXX

suspension was allowed to stir for 10 min before all volatiles were again vacuum transferred into the collection flask. After completion of the vacuum transfer, the flask was sealed and warmed to room temperature. Solvent was removed in vacuo, and the remaining residue was dissolved in H_2O (1 mL). An aliquot of this solution (20 μL) was then analyzed for the presence of NH_3 (trapped as $[NH_4][Cl]$) via the indophenol method.[38] Quantification was performed with UV−vis spectroscopy by analyzing absorbance at 635 nm.

Standard Catalytic Procedure with $[(CP^{iPr}_3)FeN_2][K(Et_2O)_{0.5}]$ (12). $[(CP^{iPr}_3)FeN_2][K(Et_2O)_{0.5}]$ (1.9 mg, 0.0025 mmol) was dissolved in Et_2O (0.5 mL) in a small Schlenk tube equipped with a stir bar. This solution was cooled to −78 °C in a cold well inside of the glovebox. A suspension of KC_8 (14 mg, 0.100 mmol) in Et_2O (0.75 mL) was cooled to −78 °C and added to the reaction mixture with stirring. After five minutes, a similarly cooled solution of $HBAr^F_4 \bullet 2$ Et_2O (93 mg, 0.092 mmol) in Et_2O (1.0 mL) was added to the suspension in one portion with rapid stirring. Any remaining acid was dissolved in cold Et_2O (0.25 mL) and added subsequently, and the Schlenk tube was sealed. The reaction was allowed to stir for 60 min at −78 °C before being warmed to room temperature and stirred for 15 min.

For further details of catalytic runs with other precatalysts and/or modified conditions, and complete tables of results, see SI.

■ ASSOCIATED CONTENT

Ⓢ Supporting Information

Spectroscopic data for new compounds, further experimental and computational details, and additional data on catalytic runs. This material is available free of charge via the Internet at http://pubs.acs.org.

■ AUTHOR INFORMATION

Corresponding Author

jpeters@caltech.edu

Notes

The authors declare no competing financial interest.

■ ACKNOWLEDGMENTS

This work was supported by the NIH (GM 070757) and the Gordon and Betty Moore Foundation, and through the NSF via a GRFP award to S.E.C. Larry Henling and Dr. Tzu-Pin Lin are thanked for their assistance with X-ray crystallography. Jon Rittle is thanked for testing the catalytic activity of $[C^{Si}P^{Ph}_3]$-FeN_2^-.

■ REFERENCES

(1) Smil, V. *Enriching the Earth*; MIT Press: Cambridge, 2001.

(2) (a) Burgess, B. K.; Lowe, D. J. *Chem. Rev.* **1996**, *96*, 2983−3011. (b) Eady, R. R. *Chem. Rev.* **1996**, *96*, 3013−3030.

(3) Peters, J. C.; Mehn, M. P. In *Activation of Small Molecules: Organometallic and Bioinorganic Perspectives*; Tolman, W. B., Ed.; Wiley-VCH: New York, 2006; pp 81−119.

(4) Hazari, N. *Chem. Soc. Rev.* **2010**, *39*, 4044.

(5) MacLeod, K. C.; Holland, P. L. *Nat. Chem.* **2013**, *5*, 559.

(6) Crossland, J. L.; Tyler, D. R. *Coord. Chem. Rev.* **2010**, *254*, 1883.

(7) Yandulov, D. V.; Schrock, R. R. *Science* **2003**, *301*, 76.

(8) Arashiba, K.; Miyake, Y.; Nishibayashi, Y. *Nature Chem.* **2011**, *3*, 120.

(9) Weare, W. W.; Dai, X.; Byrnes, M.; Chin, J.-M.; Schrock, R. R.; Muller, P. *Proc. Natl. Acad. Sci.* **2006**, *103*, 17099.

(10) (a) Saouma, C. T.; Lu, C. C.; Peters, J. C. *Inorg. Chem.* **2012**, *51*, 10043. (b) Saouma, C. T.; Kinney, R. A.; Hoffman, B. M.; Peters, J. C. *Angew. Chem., Int. Ed.* **2011**, *50*, 1. (c) Saouma, C. T.; Muller, P.; Peters, J. C. *J. Am. Chem. Soc.* **2009**, *131*, 10358.

(11) Smith, J. M.; Lachiotte, R. J.; Pittard, K. A.; Cundari, T. R.; Lukat-Rodgers, G.; Holland, P. L. *J. Am. Chem. Soc.* **2001**, *123*, 9222.

(12) Field, L. D.; Li, H.; Magill, A. M. *Inorg. Chem.* **2001**, *48*, 5.

(13) Li, Y.; Li, Y.; Wang, B.; Luo, Y.; Yang, D.; Tong, P.; Zhao, J.; Luo, L.; Zhou, Y.; Chen, S.; Cheng, F.; Qu, J. *Nat. Chem.* **2013**, *5*, 320.

(14) Rodriguez, M. M.; Bill, E.; Brennessel, W. W.; Holland, P. L. *Science* **2011**, *334*, 780.

(15) Moret, M. E.; Peters, J. C. *J. Am. Chem. Soc.* **2011**, *133*, 18118.

(16) Yuki, M.; Tanaka, H.; Sasaki, K.; Miyake, Y.; Yoshizawa, K.; Nishibayashi, Y. *Nat. Comm.* **2012**, *3*, 1254.

(17) Lee, Y.; Mankad, N. P.; Peters, J. C. *Nat. Chem.* **2012**, *2*, 558.

(18) (a) Leigh, G. J.; Jimenez-Tenorio, M. *J. Am. Chem. Soc.* **1991**, *113*, 5862. (b) Hall, D. A.; Leigh, G. J. *J. Chem. Soc., Dalton Trans.* **1996**, 3539. (c) Gilbertson, J. D.; Szymczak, N. K.; Tyler, D. R. *J. Am. Chem. Soc.* **2005**, *127*, 10184. (d) Yamamoto, A.; Miura, Y.; Ito, T.; Chen, H. L.; Iri, K.; Ozawa, F.; Miki, K.; Sei, T.; Tanaka, N.; Kasai, N. *Organometallics* **1993**, *2*, 1429. (e) George, T. A.; Rose, D. J.; Chang, Y.; Chen, Q.; Zubieta, J. *Inorg. Chem.* **1995**, *34*, 1295. (f) Borodko, Y. G.; Broitman, M. O.; Kachapina, L. M.; Shilov, A. E.; Ukhin, L. Y. *J. Chem. Soc. D* **1971**, 1185.

(19) Einsle, O.; Tezcan, A.; Andrade, S. L. A.; Schmid, B.; Yoshida, M.; Howard, J. B.; Reese, D. C. *Science* **2002**, *297*, 1696.

(20) (a) Spatzal, T.; Aksoyoglu, M.; Zhang, L.; Andrade, S. L. A.; Schleicher, E.; Weber, S.; Rees, D. C.; Einsle, O. *Science* **2011**, *334*, 940. (b) Lancaster, K. M.; Roemelt, M.; Ettenhuber, P.; Hu, Y.; Ribbe, M. W.; Neese, F.; Bergmann, U.; DeBeer, S. *Science* **2011**, *334*, 974. (c) Lancaster, K. M.; Hu, Y.; Bergmann, U.; Ribbe, M. W.; DeBeer, S. *J. Am. Chem. Soc.* **2013**, *135*, 610. (d) Wiig, J. A.; Hu, Y.; Lee, C. C.; Ribbe, M. W. *Science* **2012**, *337*, 1672.

(21) Anderson, J. S.; Rittle, J.; Peters, J. C. *Nature* **2013**, *501*, 84.

(22) Rittle, J.; Peters, J. C. *Proc. Natl. Acad. Sci. U.S.A.* **2013**, *110*, 15898.

(23) Macbeth, C. E.; Harkins, S. B.; Peters, J. C. *Can. J. Chem.* **2005**, *83*, 332.

(24) Mankad, N. P.; Whited, M. T.; Peters, J. C. *Angew. Chem., Int. Ed.* **2007**, *46*, 5768.

(25) Moret, M.-E.; Peters, J. C. *Angew. Chem., Int. Ed.* **2011**, *50*, 2063.

(26) Bontemps, S.; Bouhadir, G.; Dyer, P. W.; Miqueu, K.; Bourissou, D. *Inorg. Chem.* **2007**, *46*, 5149.

(27) Lesueur, W.; Solari, E.; Floriani, C.; Chiesi-Villa, A.; Rizzoli, C. *Inorg. Chem.* **1997**, *36*, 3354.

(28) Bickelhaupt, F.; Jongsma, C.; de Koe, P.; Lourens, R.; Mast, N. R.; van Mourik, G. L.; Vermeer, H.; Weustink, R. J. M. *Tetrahedron* **1976**, *32*, 1921.

(29) Bielawski, M.; Olofsson, B. *Chem. Commun.* **2007**, 2521.

(30) Ciclosi, M.; Lloret, J.; Estevan, F.; Lahuerta, P.; Sanau, M.; Perez-Prieto, J. *Angew. Chem., Int. Ed.* **2006**, *45*, 6741.

(31) Schlosser, M. *Pure Appl. Chem.* **1988**, *60*, 1627.

(32) Hoffmann, R.; Bissel, R.; Farnum, D. G. *J. Phys. Chem.* **1969**, *73*, 1789.

(33) Lee, Y.; Kinney, R. A.; Hoffman, B. M.; Peters, J. C. *J. Am. Chem. Soc.* **2011**, *133*, 16366.

(34) Field, L. D.; Guest, R. W.; Vuong, K. Q.; Dalgarno, S. J.; Jensen, P. *Inorg. Chem.* **2009**, *48*, 2246.

(35) Anderson, J. S.; Moret, M.-E.; Peters, J. C. *J. Am. Chem. Soc.* **2013**, *135*, 534.

(36) Weinhold, F.; Landis, C. *Valency and Bonding: A Natural Bond Orbital Donor-Acceptor Perspective*; Cambridge University Press: Cambridge, 2005.

(37) Hills, A.; Hughes, D. L.; Jimenez-Tenorio, M.; Leigh, G. F.; Rowley, A. T. *J. Chem. Soc., Dalton Trans.* **1993**, *25*, 3041.

(38) Weatherburn, M. W. *Anal. Chem.* **1967**, *39*, 971.

(39) (a) Yang, Z.-Y.; Khadka, N.; Lukoyanov, D.; Hoffman, B. M.; Dean, D. R.; Seefeldt, L. C. *Proc. Natl. Acad. Sci. U.S.A.* **2013**, *110*, 16327. (b) Simpson, F. B.; Burris, R. H. *Science* **1984**, *224*, 1095.

(40) (a) Tard, C.; Liu, X.; Ibrahim, S. K.; Maurizio, B.; DeGioia, L.; Davis, S. C.; Yang, X.; Wang, L.-S.; Sawers, G.; Pickett, C. J. *Nature* **2005**, *433*, 610. (b) Gloaguen, F.; Rauchfuss, T. B. *Chem. Soc. Rev.* **2009**, *38*, 100. (c) Darensbourg, M. Y.; Lyon, E. J.; Smee, J. J. *Coord. Chem. Rev.* **2000**, *206−207*, 533. (d) Peters, J. W.; Lanzilotta, W. N.; Lemon, B. J.; Seefeldt, L. C. *Science* **1998**, *282*, 1853. (e) Volbeda, A.;

Charon, M.-H.; Piras, C.; Hatchikian, E. C.; Frey, M.; Fontecilla-Camps, J. C. *Nature* **1995**, *373*, 580. (f) Vincent, K. A.; Parkin, A.; Armonstrong, F. A. *Chem. Rev.* **2007**, *107*, 4366.
(41) (a) Chatt, J.; Dilworth, J. R.; Richards, R. L. *Chem. Rev.* **1978**, *78*, 589. (b) Seefeldt, L.; Hoffman, B. M.; Dean, D. R. *Annu. Rev. Biochem.* **2009**, *78*, 701. (c) Lukoyanov, D.; Dikanov, S. A.; Yang, Z.-Y.; Barney, B. M.; Samoilova, R. I.; Narasimhulu, K. V.; Dean, D. R.; Seefeldt, L. C.; Hoffman, B. M. *J. Am. Chem. Soc.* **2011**, *133*, 11655.
(42) Brookhart, M.; Grant, B.; Volpe, A. F., Jr. *Organometallics* **1992**, *11*, 3920.
(43) Wietz, I. S.; Rabinovitz, M. J. *J. Chem. Soc., Perkin Trans.* **1993**, *1*, 117.
(44) Chavez, I.; Alvarez-Carena, A.; Molins, E.; Roig, A.; Maniukiewicz, W.; Arancibia, A.; Arancibia, V.; Brand, H.; Manriquez, J. M. *J. Organomet. Chem.* **2000**, *601*, 126.
(45) Job, R.; Earl, R. *Inorg. Nuc. Chem. Lett.* **1979**, *15*, 21.
(46) Evans, D. F. *J. Chem. Soc.* **1959**, 2003.
(47) Sheldrick, G. M. *Acta Cryst. A.* **2008**, *82*, 169.
(48) Frisch, M. J.; Trucks, G. W.; Schlegel, H. B.; Scuseria, G. E.; Robb, M. A.; Cheeseman, J. R.; Montgomery, Jr., J. A.; Vreven, T.; Kudin, K. N.; Burant, J. C.; Millam, J. M.; Iyengar, S. S.; Tomasi, J.; Barone, V.; Mennucci, B.; Cossi, M.; Scalmani, G.; Rega, N.; Petersson, G. A.; Nakatsuji, H.; Hada, M.; Ehara, M.; Toyota, K.; Fukuda, R.; Hasegawa, J.; Ishida, M.; Nakajima, T.; Honda, Y.; Kitao, O.; Nakai, H.; Klene, M.; Li, X.; Knox, J. E.; Hratchian, H. P.; Cross, J. B.; Bakken, V.; Adamo, C.; Jaramillo, J.; Gomperts, R.; Stratmann, R. E.; Yazyev, O.; Austin, A. J.; Cammi, R.; Pomelli, C.; Ochterski, J. W.; Ayala, P. Y.; Morokuma, K.; Voth, G. A.; Salvador, P.; Dannenberg, J. J.; Zakrzewski, V. G.; Dapprich, S.; Daniels, A. D.; Strain, M. C.; Farkas, O.; Malick, D. K.; Rabuck, A. D.; Raghavachari, K.; Foresman, J. B.; Ortiz, J. V.; Cui, Q.; Baboul, A. G.; Clifford, S.; Cioslowski, J.; Stefanov, B. B.; Liu, G.; Liashenko, A.; Piskorz, P.; Komaromi, I.; Martin, R. L.; Fox, D. J.; Keith, T.; Al-Laham, M. A.; Peng, C. Y.; Nanayakkara, A.; Challacombe, M.; Gill, P. M. W.; Johnson, B.; Chen, W.; Wong, M. W.; Gonzalez, C.; and Pople, J. A. *Gaussian 03, Revision C.02*; Gaussian, Inc., Wallingford CT, 2004.